Structures 48 (2023) 2048–2061

Contents lists available at ScienceDirect

Structures

journal homepage: www.elsevier.com/locate/structures

Determination of stress-strain relationship based on alkali activator ratios in geopolymer concretes and development of empirical formulations

Ahmet Özbayrak [a,*], Hurmet Kucukgoncu [b], Oguzhan Atas [c], Huseyin Hilmi Aslanbay [a], Yuksel Gul Aslanbay [a], Fatih Altun [a]

[a] Erciyes University, Engineering Faculty, Civil Engineering Department, Kayseri, Türkiye
[b] Abdullah Gül University, Engineering Faculty, Civil Engineering Department, Kayseri, Türkiye
[c] Alanya Alaaddin Keykubat University, Engineering Faculty, Civil Engineering Department, Antalya, Türkiye

ARTICLE INFO

Keywords:
Geopolymer concrete mixtures
Alkali activator ratios
Mechanical properties
Traditional concrete models
Regression analysis
Empirical formulations

ABSTRACT

Fly ash-based geopolymer has recently gained attention of researchers due to its potential application, as well as being an alternative binder with low emissions compared to ordinary Portland cement (OPC) in concrete production. Studies which are conducted on the design and mechanical properties of structural members produced from fly ash geopolymer concrete (GPC) are very important in terms of increasing the use of this concrete. The aim of this study is to obtain experimental data on the effect of sodium silicate/sodium hydroxide (SS/SH) and alkali activators/fly ash (AA/FA) ratios on the mechanical properties of a low calcium heat-cured fly ash geopolymer. In addition, it is to reveal the similarities and differences of OPC and GPC by comparing the mathematical formulations in existing regulations and concrete models with experimental data. Thus, geopolymer cylinder concrete samples were produced using 15 different mixtures with SS/SH ratios of 1.5, 2.5 and 3.5, while AA/FA ratios of 0.4, 0.5, 0.6, 0.7 and 0.8. At the end of the study, the optimum SS/SH ratio was obtained as 2.5. A decrease in the AA/FA ratio increases the compressive and splitting tensile strength, while an increment increases the ductility and consuming energy. In addition, the relationship between the experimental data and the splitting tensile strength and modulus of elasticity formulations depending on the compressive strength given in other studies and regulations as a part of literature was investigated, and then, two alternative empirical formulations considering the ratios of alkali activators were proposed at the end of the regression analysis. When the stress-strain relationship of OPC concrete models and GPC mixtures were compared, the closest unconfined concrete model for GPC concrete was the Hognestad model.

1. Introduction

The demand for concrete increases exponentially today as the construction increases day by day. The production of Portland cement concrete increases the emission of CO_2, which has an important role in increasing the effect of greenhouse gasses in the atmosphere. For this reason, research on the use of fly ash material in the waste product class in concrete production is important in terms of making concrete more environmentally friendly. Studies conducted in recent years reveal that geopolymer concrete (GPC) has superior properties compared to ordinary Portland cement concrete (OPC).

Fly ash (FA) produced from coal-fired power plants, which are known to significantly improve the mechanical and strength properties of GPC, are the most widely preferred aluminosilicate binders [1]. The presence of silica and alumina oxides in GPC is generally explained by the silica/alumina (SiO_2/Al_2O_3) ratio. Due to increase in silica alumina ratio, the compressive strength of FA-based GPC increases [2]. In general, it has been determined that the compressive strength increases with the increase of the FA content (254 to 670 kg/m^3) in the geopolymer concrete mixture, while the fly ash with fine and glassy phase is more reactive in most of the studies [3].

The composition and amount of silicate/hydroxide, activator/binder, Si/Al and Na_2O/SiO_2 ratios are the main factors which affect the polymeric chains in the geopolymerization reaction [4]. The most common activators used for the preparation of GPC are a combination of Na_2SiO_3 and NaOH [5,6]. The effects of activators on the polymerization process are important. Polymerization occurs at a high rate when alkali activators dissolve Si and Al from the binder material to form an

* Corresponding author.
E-mail address: ozbayrak@erciyes.edu.tr (A. Özbayrak).

https://doi.org/10.1016/j.istruc.2023.01.104
Received 11 October 2022; Received in revised form 16 January 2023; Accepted 19 January 2023
Available online 27 January 2023

N—A—S—H gel matrix. Activators prepared by using NaOH and Na_2SiO_3 improve the reactivity in fly ash [7,8]. It has been observed by many researchers [9–13] that alkaline activators are the main factor which influence the strength development of GPC. According to these studies, the effect of activator/binder and silicate/hydroxide ratios play an important role in the geopolymerization process. The most commonly used activators in GPC are Na_2SiO_3 and NaOH. Na_2SiO_3 and NaOH doped GPC samples show better mechanical, strength and microstructural properties [14]. Using only hydroxides as activators in GPC occurs pores and shrinkage cracks that lead to poor mechanical properties due to hydroxides only help dissolve precursor Si and Al ions. However, the inclusion of a source of hydroxide and a source of silicate as activator increases the fluidity of GPC [15–17]. While the excessive use of silicates in GPC inhibits geopolymerization, excess hydroxide leads to early and vigorous precipitation of aluminosilicate precursors, which inhibits further formation of the geopolymer gel [18]. Vora et al. [19] investigated the effects of curing temperature, Na_2SiO_3/NaOH and alkali activator/fly ash ratios on the compressive strength of GPC. It was determined that the compressive strength increased with the increase in curing temperature, and the compressive strength decreased with the increase in the Na_2SiO_3/NaOH ratio and the alkali activator/FA ratio. In addition, the dissolution of silicon and aluminum particles in the geopolymerization process depends on the molarity of NaOH. The higher the molarity of NaOH, the higher the dissolution of silicon and aluminum particles and, consequently, the higher the compressive strength of GPC mixtures. As the molarity of NaOH is higher, the dissolution of silicon and aluminum particles increase and, consequently, the compressive strength of GPC mixtures increases [20]. The optimum compressive strength of GPC was observed at 14 M NaOH concentration, which can be attributed to the complete dissolution of silicon and aluminum particles in the geopolymerization process [21]. However, it was observed that the GPC mixtures became sticky and the workability of GPC decreased because of the increase of NaOH molarity. It is figured out that water content plays an important role in the dissolution of ions in the geopolymerization process [22]. Chithambaram et al. [23] obtained the highest compressive strength at 14 M and 90 °C with increasing NaOH molarity and curing temperature and observed that the compressive strength decreased at lower temperatures and higher NaOH molarities. The literature shows that GPC has a lower modulus of elasticity than OPC concrete for a given compressive strength [24–26].

Many experimental and theoretical studies have been carried out by different researchers and various behavior models have been proposed in order to determine the behavior of OPC unconfined concrete. In line with these studies, the ductility and the strain behavior of reinforced concrete members constructed by the use of traditional concrete and reinforcement together are calculated approximately by using moment curvature analysis. The developed models provide great convenience especially in the section design and analysis of the members [27]. One of the first models developed according to the unconfined concrete behavior is the Hognestad concrete model [28]. It was followed by Kent-Park, Mander, Saatcioglu-Razvi unconfined concrete models [29–32]. Some empirical formulations are proposed for the calculation of compressive strength, flexural strength, splitting tensile strength and modulus of elasticity of GPC concrete samples [33–36]. However, there are very few studies proposing a mathematical concrete model for the entire stress-strain curve. Srivathsav et al. [37] compared the stress strain curves obtained from the tests for traditional concrete samples (OPC) in concrete class M20 and geopolymer concrete samples (GPC) in concrete class G20 according to the Indian regulations with the empirical equations of the modified Saenz model. They concluded that the graphs show a similar trend. Wang et al. [38] compared the stress-strain curves of different alkali-activated geopolymer concretes and traditional concretes for 3 different concrete strengths by obtaining them with the help of various empirical formulations within the framework of Chinese regulation GB/T 50010–2010. By this comparison, it has been revealed that there is no significant difference in the ascending curves of the stress-strain graphs of all these different concretes whereas there are significant differences in the descending curves. These studies in the literature consider the models developed according to GPC concrete classes and strengths prepared only within the framework of limited regulations. In a more general context, a study that takes into account the concrete classes for all regulations has not been carried out yet. Therefore, in this study, stress-strain graphs of GPC concrete samples were obtained by using some of the commonly used mathematical concrete models for traditional unconfined concrete considering all strength classes which are independent from the regulations. Comparing these graphs with the graphs obtained from the experimental data, the availability of these models used for OPC concrete was also investigated for GPC concrete.

The scope of this study is to obtain experimental data on the effect of sodium silicate/sodium hydroxide (SS/SH) and alkali activators/fly ash (AA/FA) ratios on the mechanical properties of low calcium fly ash geopolymer. Besides, it is aimed to reveal the similarities and differences of OPC and GPC by comparing existing regulations and concrete models with experimental data. For this purpose, modulus of elasticity and splitting tensile strength values were calculated by using some empirical formulations given in the literature and regulations and then, experimental results were compared with these calculations. In addition, empirical formulations have been developed for both the modulus of elasticity and the splitting tensile strength, as a result of the regression analysis performed by considering the alkali activator mixture ratios and the compressive strengths. By comparing the concrete models in the literature for OPC concrete with the stress-strain curves obtained from the experimental data, it has been investigated whether it can be used for geopolymer concretes as well. Also, the energy consumption capacities of the geopolymer concrete samples were obtained by calculating the areas under the curves obtained. Thus, compressive strength, modulus of elasticity, splitting tensile strength and energy consumption capacity of geopolymer concrete samples were calculated according to different mixing ratios and the effect of mixing ratios on these values was revealed.

2. Experimental program

2.1. Materials

Different GPCs have different effects depending on the alumina and silica content in the aluminosilicates used in the geopolymer. Besides, the performance of an aluminosilicate mostly depends on the optimum percentage of silica and alumina in the chain reaction of the geopolymerization process [39]. The fly ash used in this study was obtained from Isken Sugözü Power Plant with low calcium and is Class F according to ASTM C618 [40]. The color of the fly ash is dark green, and the specific gravity measured by using the Blaine Air Permeability method is 2.32 g/cm^3 [41]. The chemical composition of the fly ash-based aluminosilicate used in the study is as given in Table 1.

Table 1
Chemical components of fly ash.

Components	%
SiO_2, 1	55.9
Al_2O_3, 2	20.7
Fe_2O_3, 3	9.31
Sum of 1, 2, 3	85.9
CaO	3.98
MgO	2.33
SO_3	0.33
Na_2O	1,35
K_2O	2.19
Cl-	0.05
LOI (loss of ignition)	2.22
Fineness (>45 μm)	17.4

A mixture of NaOH and Na_2SiO_3 was preferred as the alkaline activator solution. NaOH grains in pallet form used to prepare 14 M sodium hydroxide solution are 98 % pure. The NaOH solution was left at room temperature for at least 24 h before use. The ratios of the components in the Na_2SiO_3 solution are $Na_2O = 14.41$ %, $SiO_2 = 29.64$ %, $H_2O = 55.73$ % and the bulk density is 1510 kg/m^3. Crushed stone with a diameter of 7–14 mm was used as coarse aggregate and river sand with a diameter of 3–4 mm was used as fine aggregate. In order to reduce the absorption of water and chemicals, the moisture content of the fine and coarse aggregates is adjusted as close to the saturated dry surface as possible.

2.2. Mix proportions

Alkaline enrichment in GPC significantly affects the samples with less water/binder ratio by increasing the shrinkage of the mortar system and the development of the pore structure and causes deterioration of the mechanical strength [42,43]. Therefore, the amounts of alkaline activators should be well mixed in the correct proportions when designing the GPC mix. The formulations with different alkali activator ratios used in the study are given in Table 2.

2.3. Mixing and casting

Firstly, coarse and fine aggregate with a saturated dry surface and fly ash were mixed for 2 min for the production of concrete mortar. After the Na_2SiO_3 solution, one of the alkali activators, was completely poured into the mixture, the NaOH solution prepared 24 h before was added to the mixture slowly for 5 min. After a total of 8 min, no extra water or plasticizer was added to the mixture. The concrete mixture was casted in Ø100x200 mm cylinder molds by compacting at three stages. Each of the test samples given in Table 2 were produced as 4 numbers, three of which were used in the compression test while one in the splitting tensile test.

The manufactured samples were cured in the mold at a constant 90° C in the oven for 24 h after casting. Afterwards, the samples removed from the molds were stored at room temperature for 28 days until strength tests. Within the scope of the research, a total of 60 cylinder samples in 15 different formulas were produced (Fig. 1).

The workability of fresh concrete varies depending on the AA/FA ratio. The mean values in the slump test were measured as 18.6 cm for AA/FA ratio 0.4, 19.8 cm for 0.5, 21.2 cm for 0.6, 22.4 cm for 0.7 and 23.6 cm for 0.8, respectively. The setting time of fresh concrete varies depending on the ratio of AA/FA and SS/SH. For the SS/SH ratio of 1.5, when the AA/FA ratio increased from 0.4 to 0.8, the time was increased by another 5 min and the setting time was measured between 10 and 15 min. For the SS/SH ratio of 2.5, when the AA/FA ratio increased from 0.4 to 0.8, the time was increased by another 10 min and the setting time was measured between 15 and 25 min. For the SS/SH ratio of 3.5, when the AA/FA ratio increased from 0.4 to 0.8, the time was increased by 95 min and the setting time was measured between 25 and 120 min.

Table 2
Formulations and mixture amount of test samples (kg/m^3).

Sample No	Sample Name	FA	SS	SH	Fine Aggregate	Coarse Aggregate
1	A1.5W0.4	406	97	65	643	1194
2	A1.5W0.5	406	122	81	643	1194
3	A1.5W0.6	406	146	97	643	1194
4	A1.5W0.7	406	171	114	643	1194
5	A1.5W0.8	406	195	130	643	1194
6	A2.5W0.4	406	116	46	643	1194
7	A2.5W0.5	406	145	58	643	1194
8	A2.5W0.6	406	174	70	643	1194
9	A2.5W0.7	406	203	81	643	1194
10	A2.5W0.8	406	232	93	643	1194
11	A3.5W0.4	406	126	36	643	1194
12	A3.5W0.5	406	158	45	643	1194
13	A3.5W0.6	406	189	54	643	1194
14	A3.5W0.7	406	221	63	643	1194
15	A3.5W0.8	406	253	72	643	1194

FA: Fly Ash, SS: Sodium Silicate Solution (Na_2SiO_3), SH: Sodium Hydroxide Solution (NaOH).

2.4. Test setup

During the cylinder compressive strength test, the stress-strain behavior was calculated with the help of a compressometer. The average of two potentiometer measurements was used to determine the longitudinal deformation. The load values were determined by the load cell placed under the cylinder sample. The measured values were transferred to the computer with the help of a data logger (Fig. 2).

2.5. Test variables

Na_2SiO_3/NaOH (SS/SH) ratios were selected as 1.5, 2.5 and 3.5, respectively based on previous research [44–49]. Al Bakri et al. [50] obtained the highest compressive strength from samples with SS/SH ratio of 2.5 and AA/FA ratio of 0.5. Accordingly, alkali activator/fly ash (AA/FA) mixing ratios were used as 0.4, 0.5, 0.6, 0.7 and 0.8 considering the workability in the study. As ratios, the values below 0.4 were not preferred because they were too solid to be processed and those above 0.8 were liquid at a level that would cause separation [51]. The mixing ratios of the chemicals that carry out the geopolymerization process are given in Table 3.

The dissolution of silica and alumina in the geopolymerization process that constitutive the aluminosilicate gel is very important to determining the stability of the geopolymer during the hardening process, which contributes to the high compressive strength of the geopolymer. The ratios affecting the dissolution of silica and alumina were chosen as variables in this study. No water was added to the mixture other than the specified ratios.

2.6. Mathematical model for stress- strain behavior

For concrete models, empirical formulations have been developed by using experimental data and models that determine the σ-ε relationship of OPC concrete are proposed in order to find out the behavior. Thus, the σ-ε curves obtained from the test results are idealized and simplified in order to facilitate the mathematical solution. Idealized and simplified σ-ε curves are called “mathematical models” [27].

Stress-strain relations (Table 4) of Hognestad, Kent-Park, Mander, Saatcioglu-Razvi unconfined concrete models, which are the most widely used as unconfined concrete models in the literature, were used in the study. Stress-strain graphs were obtained from experimental results of GPC concrete of compressive strength tests of 15 groups with different mixing ratios. The equations of the concrete models used are given as follows [29–32].

σ-ε curves were drawn for each concrete model by using the above equations. The amounts of consumed energy were obtained by calculating the areas under the stress-strain curves for each model relation. The amount of energy consumed by concrete samples under load is expressed as a measure of ductility. Thus, the relationship between the amount of energy consumed, which is an important parameter in terms of building elements, is revealed by using experimental data and concrete models.

2.7. Analytical formulations for splitting tensile stress and modulus of elasticity

According to studies and regulations in the literature, the modulus of elasticity has a direct relationship with the compressive strength [21,52,53]. However, the density is also taken into account in some regulations and studies [54,55]. In addition to the compressive strength,

Fig. 1. Manufacture of cylinder samples.

Fig. 2. Experimental set up for compressive strength test.

Table 3
Mixing ratios of chemicals for test samples.

Sample No	Sample Name	SS/SH	AA/FA	Na_2O/SiO_2	SiO_2/Al_2O_3	W/FA
1	A1.5W0.4	1.50	0.40	0.18	3.03	0.25
2	A1.5W0.5	1.50	0.50	0.22	3.12	0.30
3	A1.5W0.6	1.50	0.60	0.25	3.20	0.36
4	A1.5W0.7	1.50	0.70	0.28	3.29	0.42
5	A1.5W0.8	1.50	0.80	0.31	3.38	0.47
6	A2.5W0.4	2.50	0.40	0.16	3.10	0.25
7	A2.5W0.5	2.50	0.50	0.19	3.20	0.30
8	A2.5W0.6	2.50	0.60	0.22	3.30	0.36
9	A2.5W0.7	2.50	0.70	0.24	3.40	0.42
10	A2.5W0.8	2.50	0.80	0.26	3.51	0.47
11	A3.5W0.4	3.50	0.40	0.15	3.14	0.25
12	A3.5W0.5	3.50	0.50	0.17	3.25	0.30
13	A3.5W0.6	3.50	0.60	0.20	3.36	0.36
14	A3.5W0.7	3.50	0.70	0.22	3.47	0.42
15	A3.5W0.8	3.50	0.80	0.24	3.58	0.47

FA: Fly Ash, SS: Sodium Silicate Solution (Na_2SiO_3), SH: Sodium Hydroxide Solution (NaOH), AA: Alkali Activator Solution (Na_2SiO_3 + NaOH), W: Water.

the Na_2SiO_3/NaOH (SS/SH) ratio of alkaline activators and the ratio of alkaline activators to fly ash (AA/FA) were considered in the study. While the modulus of elasticity increased with the increase in compressive strength, the increase in the ratio of alkaline solutions decreased the modulus of elasticity. Therefore, a regression analysis was performed in accordance with the relationship between the modulus of elasticity, the compressive strength and the ratios (SS/SH) and (AA/FA). By using the equation developed from this result, the results obtained

Table 4
Empirical formulations for obtaining stress-strain curves.

Concrete Model	Parabolic Curve	Linear Curve	No
Hognestad (1951)	$\sigma_c = f_c[\frac{2\varepsilon_c}{\varepsilon_{c0}} - \left(\frac{\varepsilon_c}{\varepsilon_{c0}}\right)^2]$ $\varepsilon_{co} = \frac{2f_c}{E_c}$ $E_c = 12680 + 460 \times f_c$	$\sigma_c = 0.85 \times f_c$	(1)
Kent-Park (1971)	$\sigma_c = f_c[\frac{2\varepsilon_c}{\varepsilon_{c0}} - \left(\frac{\varepsilon_c}{\varepsilon_{c0}}\right)^2]$	$\sigma_c = f_c[1 - Z_u(\varepsilon_c - \varepsilon_{c0})]Z_u = \frac{0.5}{\varepsilon_{50u-\varepsilon_{c0}}}$ $\varepsilon_{50u} = \frac{3 + 0.29f_c}{145f_c - 1000}$	(2)
Mander (1988)	$\sigma_c = \frac{f_{co}xr}{r - 1 + x^r}$ $x = \frac{\varepsilon_c}{\varepsilon_{c0}}r = \frac{E_c}{E_c - E_{sec}}$ $E_{sec} = \frac{f_{co}}{\varepsilon_{c0}}E_c = 5000 \times \sqrt{fc}$	$\sigma_c = f_{co}(\frac{2r}{r - 1 + 2^r})$ $x = \frac{\varepsilon_c}{\varepsilon_{c0}}r = \frac{E_c}{E_c - E_{sec}}$ $E_{sec} = \frac{f_{co}}{\varepsilon_{c0}}E_c = 5000 \times \sqrt{fc}$	(3)
Saatcioglu-Razvi (1992)	$\sigma_c = f_c[\frac{2\varepsilon_c}{\varepsilon_{c0}} - \left(\frac{\varepsilon_c}{\varepsilon_{c0}}\right)^2]$	$\sigma_c = f_{c+}(\frac{f_c - f_{c85}}{\varepsilon_{c0} - \varepsilon_{c85}})(\varepsilon_c - \varepsilon_{c0})$	(4)

σ_c: compressive stress of concrete; f_c: longitudinal concrete stress; f_{co}: compressive strength of unconfined concrete.
f_c85: 85 % of longitudinal stress; ε_c = longitudinal concrete strain; ε_{co} = strain at maximum stress fco of unconfined concrete; εc85: strain at 85 % of maximum stress of unconfined stress ε50u: strain at 50 % εu85: strain at %85 strength levels beyond the peak; E_c: modulus of elasticity of concrete; E_{sec} = secant modulus of unconfined concrete at peak stress.

from the experimental data and analytical formula were calculated as percent error value for each group of geopolymer concrete samples. By using the equation developed, the results obtained from the experimental data and empirical formulations were calculated as percentage error value for each group of geopolymer concrete samples.

Similarly, regression analysis was performed for splitting tensile strength and a strength formulation was developed in accordance with the model that was designed at the end of the analysis. The independent variable in this formulation is not only the compressive strength, but also the ratios of alkaline solutions (SS/SH) and (AA/FA) are taken into account in the formulation as an independent variable, slightly different from what is expressed in the studies and regulations in the literature [56,57]. Accordingly, splitting tensile strengths developed for geopolymer samples of 15 different groups in total were calculated analytically and compared with experimental data and some other formulations given in the literature.

R^2, standard error values were calculated in order to determine to what extent the equations produced according to the results of the regression analysis of both the modulus of elasticity and the splitting tensile strength are compatible with the dependent and independent variables, that is, the performance of the model. The P value was calculated to reveal the correlation between the variables, that is, whether the changes in the variables affect each other. The fact that this value is less than 0.05 indicates that there is a correlation between the variables. The standard error, on the other hand, is a criterion that shows the distribution of the means of samples of the same size to be selected from the same population and is obtained by dividing the standard deviation value by the square root of the number of subjects. The standard error of the mean refers to the variation of the mean in the distribution and decreases with increasing sample size. The low standard error value is crucial for estimating the population parameter and finding out a narrower confidence interval [58]. The correlation coefficient R is the coefficient indicating the direction and size of the relationship between the independent variables and takes a value range from −1 to +1. As this value diverges from zero and converges to 1 or −1, this indicates that the correlation between the variables is so good. According to Cohen (1988), this value is ± 0.50 or above; it indicates that there is a high correlation between these variables [59]. The determination coefficient R^2 is defined as the ratio of the explained variation to the total variation. It is a measure of the goodness of the regression model which fits the dependent and independent variables. This value is between 0 and 1, and as it gets closer to 1, it shows that the fitness between the variables increases [58].

3. Result and discussions

3.1. Compressive strength

Cylinders with dimensions of Ø100x200 mm were used for ASTM C39 compressive strength tests [60]. The expression “A” denotes the ratio of alkali activators to each other Na_2SiO_3/NaOH (SS/SH) whereas the expression “W” is the ratio of alkali activators to fly ash (AA/FA). The compressive strengths of the mixtures in which low calcium fly ash is activated with activators at different rates are given in Fig. 3.

The highest strength is the A1.5W0.5 mix. When the ratio of alkaline solutions increased the strength decreased. The lowest compressive strengths were obtained from the samples with SS/SH ratio of 3.5. According to AA/FA, the highest average strength was obtained from 0.5 ratio, and the lowest strength average was 0.8 ratio. According to SS/SH, the highest average strength was obtained from 2.5 ratio, and the lowest average strength from 3.5 ratio.

During the experimental study, segregation started with the AA/FA ratio exceeding 0.6. This became more evident when the ratio increased to 0.7 and 0.8. The amount of water ratio increased with the increase in alkaline activator solution. This may decrease the strength by causing an increase in the pore structure of the concrete.The compressive strength of geopolymer concrete is inversely proportional to the water/geopolymer binder ratio. The compressive strength of geopolymer concrete decreases with increase in water to geopolymer binder ratio. It is informed that the optimal value of water to binder ratio varies from 0.25 to 0.35 for geopolymer concrete. Higher ratio leads to segregated mix, whereas lower ratio causes viscous and dry a geopolymer concrete mix [61]. When the mechanical and physical properties of the geopolymer concrete are evaluated in terms of the water/binder ratio, alkaline activator to fly ash ratios of 0.7 and 0.8 are out of these values. It explains one reason for the segregation in the geopolymer process with AA/FA ratios of 0.7 and 0.8.

A slight increase in the alkali activator content provides a high activation of the fly ash, and it produces a highly reacted dense aluminosilicate gel matrix. In this case, it indicates an improvement in the compressive strength. However, excessive increase in the amount in the mixture leads to the inhibition of the geopolymerization process and reduces the compressive strength. Therefore, there is a large number of unreacted or partially reacted silicate phases in the geopolymer matrix. However, an increase in the AA/FA ratio causes an increase in porosity, especially in mixtures cured at high temperatures. As a result of all these reasons, the compressive strength of geopolymer concrete decreases. Hadi et al. reported that the alkali activator ratio required to obtain

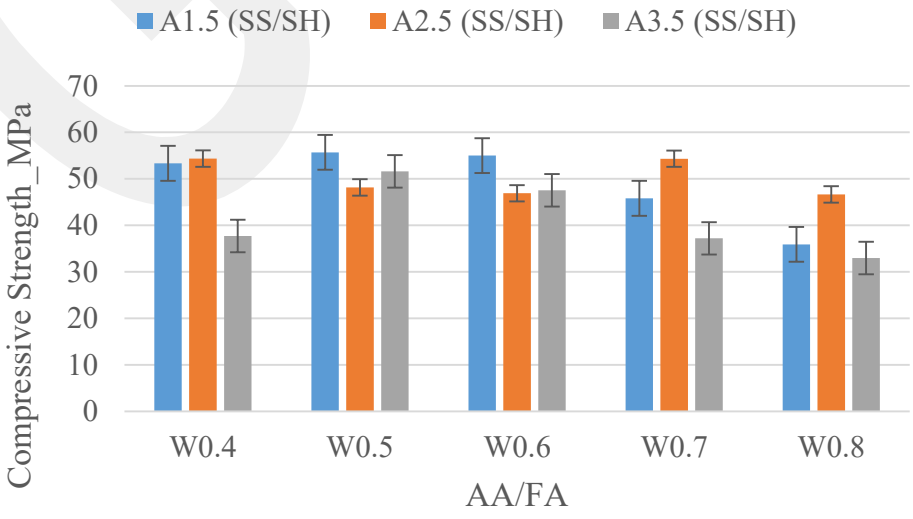

Fig. 3. Compressive strength of mixtures using solutions in different ratios.

optimum compressive strength is 0.5 and 0.6 according to the amorphous component content and particle size of the fly ash in the mixture. Accordingly, each type of mixture has an optimum AA/FA ratio required to achieve the high compressive strength. In the study, this ratio was obtained as 0.5 [62].

3.2. Splitting tensile strength

Cylinders samples with dimensions of Ø100x200 mm were used for ASTM C496 splitting tensile strength tests, respectively [63]. The tensile strength of conventional concrete varies between 10 and 15 % of its compressive strength [64]. Experimental data, the equations proposed in different regulations, and modulus of elasticity values calculated from previous research articles in the literature are compared in Table 5. The splitting tensile strength values were calculated by using Eqs. (5) and (6) with respect to ACI363-R92, CEB-FIP, respectively [65,66]. In addition, the modulus of elasticity for geopolymer concrete was calculated by using the Eqs. (7) to (10) suggested by some researchers [67–70].

ACI 363-R92

$$f_{sp} = 0.59 \times \sqrt{f_c} \tag{5}$$

CEB-FIB

$$f_{sp} = 0.301 \times (f_c)^{0.67} \tag{6}$$

Gardner et al.

$$f_{sp} = 0.6 \times (f_c)^{2/3} \tag{7}$$

Raphael et al.

$$f_{sp} = 0.2 \times (f_c)^{0.7} \tag{8}$$

De Larrard et al.

$$f_{sp} = 0.6 + 0.06 \times (f_c) \tag{9}$$

Ryu et al.

$$f_{sp} = 0.17 \times (f_c)^{3/4} \tag{10}$$

The highest splitting tensile strength was obtained from the A2.5W0.5 mix in the study. When the ratio of alkaline solutions increased, the compressive strength decreased. According to AA/FA, the highest average strength was obtained from 0.5 ratio, and the lowest strength average was 0.8 ratio. With respect to SS/SH, the highest average strength was obtained from 2.5, and the lowest average strength from 3.5 in this study. Splitting tensile strengths of mixtures in which heat-cured fly ash is activated with activators at different ratios are given in Fig. 4.

As seen, only the compressive strength is taken into account in all the formulations used in the literature for the calculation of splitting tensile strength. However, it is observed from the calculations obtained by using the equations in Table 5 and the graphs plotted from the experimental data in Fig. 5 that the alkali activator solution ratios also have an effect on the splitting tensile strength of the geopolymer concrete samples. Therefore, an empirical formulation is proposed in the study that considers not only the compressive strength but also the alkali activator ratios (SS/SH) and (AA/FA) used as an independent variable. The results obtained by using the formulation in Equation (11) are given in Fig. 5.

$$f_{sp} = \sqrt{0,0041 \times f_c^2 + 10.485 \times \left[\left(\frac{SS}{SH}\right) \Big/ \left(\frac{AA}{FA}\right)\right]^{0.295}} \tag{11}$$

The correlation coefficient R, the determination coefficient R^2, the standard error and P values are calculated in order to check the accuracy of the regression model and whether the variables are related to each other, and they are given in Table 6. As observed from the model, the P values for the independent variables remained below 0.05. The correlation coefficient is very close to 1 as the value of R 0.98 and also the determination coefficient R^2 equals to 0.96 [34,59].

It is found out from the Root Mean Squared Error (RMSE) values calculated for all groups in Table 7 that the model proposed in the study gives results closer to the experimental data than other models in the literature. It is seen that the proposed formulation gives close results and the use of alkali solution ratios in the formulation improves the calculated values numerically [59].

3.3. Modulus of elasticity

Modulus of elasticity is an important mechanical property showing the linear strength of concrete material and is determined according to ASTM standard C469M-14 [71]. It is reported that kiln-cured fly ash-based geopolymer samples have lower modulus of elasticity values compared to traditional concrete [72,73]. Experiments have shown that the modulus of elasticity values of kiln-cured fly ash-based geopolymer concrete samples with an average compressive strength of approximately 55 MPa are between 14.9 % and 28.8 % compared to traditional concrete [74].

Experimental data, equations given in different regulations, and modulus of elasticity values calculated from some previous studies in literature are compared in Table 8. Hence, the modulus of elasticity was calculated by using Eqs. (12) to (14) according to ACI318-14, CEB-FIP and TS 500–2000, respectively [54,66,75]. Also, the modulus of elasticity for geopolymer concrete was calculated by using the Eqs. (15) to (19) proposed by some researchers [21,36,52,53,55].

ACI 318–14

$$E_c = 0.043 \times \rho^{1.5} \times \sqrt{f_c} \tag{12}$$

CEB-FIB

Table 5
Splitting tensile strength of GPC from regulations, literature and experimental study (MPa).

Sample Name	ACI363 R-92	CEB-FIB Model	Gardner et al.	Raphael et al.	De Larrard et al.	Ryu et al.	Experimental (28 Days)
A1.5W0.4	4,31	4,32	8,50	3,24	3,80	1,24	5,70
A1.5W0.5	4,35	4,38	8,61	3,28	3,86	1,25	4,84
A1.5W0.6	3,62	3,43	6,75	2,54	2,86	1,04	5,55
A1.5W0.7	4,40	4,45	8,75	3,34	3,94	1,27	4,83
A1.5W0.8	4,09	4,04	7,94	3,01	3,49	1,18	4,34
A2.5W0.4	4,24	4,23	8,32	3,16	3,70	1,22	4,98
A2.5W0.5	4,38	4,41	8,68	3,31	3,90	1,26	6,19
A2.5W0.6	4,04	3,97	7,80	2,96	3,41	1,16	4,77
A2.5W0.7	4,07	4,00	7,87	2,98	3,45	1,17	5,34
A2.5W0.8	3,99	3,90	7,68	2,91	3,35	1,15	4,34
A3.5W0.4	4,35	4,38	8,61	3,28	3,86	1,25	4,78
A3.5W0.5	3,60	3,40	6,69	2,51	2,83	1,04	4,91
A3.5W0.6	3,54	3,32	6,53	2,45	2,75	1,02	4,72
A3.5W0.7	4,03	3,95	7,77	2,95	3,40	1,16	5,37
A3.5W0.8	3,39	3,13	6,17	2,31	2,58	0,98	4,53

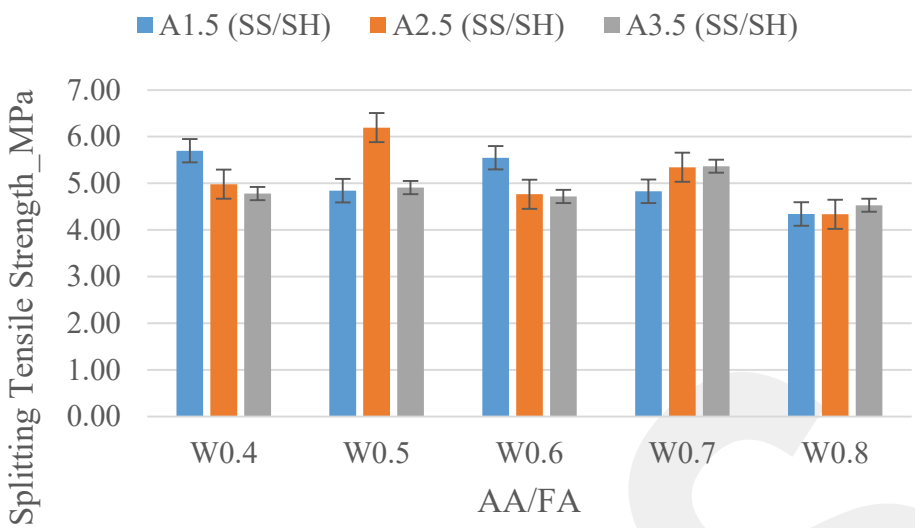

Fig. 4. Splitting tensile strength of mixtures using different ratios of solution.

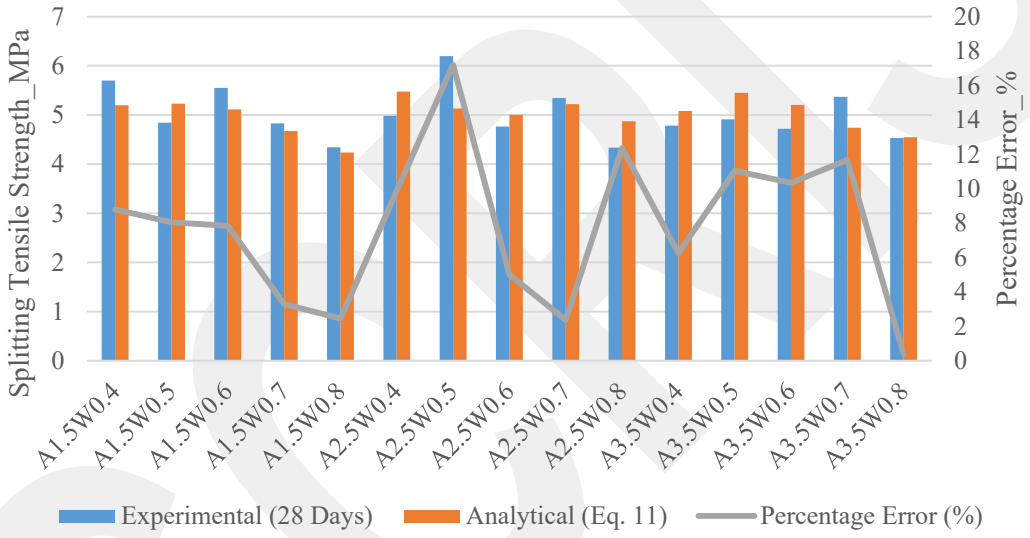

Fig. 5. Comparison of experimental and numerical strengths and percentage error values.

Table 6
Regression statistics values obtained for the splitting tensile strength formula.

Regression Statistics	Values
Correlation Coefficient R	0.98
Determination Coefficient, R^2	0.96
Standard Error	5.38
P-value of Strength	0.048
P-value of Alkali Solution	0.003
Sample Number	15

Table 7
RMSE values calculated by considering the error values of all samples of the empirical formulations used in the splitting tensile strength calculation.

Splitting Tensile Strength	Gardner et al.	Raphael et al.	De Larrard et al.	Ryu et al.	In this study
RMSE	58,41	41,43	32,78	76,76	5.02

$$E_c = 0.85 \times 2.15 \times 10^4 \times \sqrt[3]{\frac{f_c}{10}} \quad (13)$$

TS500-2000

$$E_c = 3250 \times \sqrt{f_c} + 14000 \quad (14)$$

Diaz Loya et al.

$$E_c = 0.037 \times \rho^{1.5} \times \sqrt{f_c} \quad (15)$$

Hardjito et al.

$$E_c = 2707 \times \sqrt{f_c} + 5300 \quad (16)$$

Lee-Lee

$$E_c = 5300 \times \sqrt[3]{f_c} \quad (17)$$

Nath-Sarker

$$E_c = 3510 \times \sqrt{f_c} \quad (18)$$

Reddy-Muniraj

$$E_c = 3282 \times \sqrt{f_c} \quad (19)$$

Table 8
Modulus of elasticity of GPC from regulations, literature and experimental study (MPa).

Sample Name	*ACI* 318–14	CEB-FIB Model	TS 500–2000	Diaz Loya et al.	Hardjito et al.	Lee-Lee	Nath-Sarker	Reddy-Muniraj	Experimental (28 Days)
A1.5W0.4	35,386	31,929	37,734	30,448	25,068	19,950	25,633	23,968	22,896
A1.5W0.5	36,096	32,395	38,256	31,059	25,503	20,241	26,197	24,495	22,854
A1.5W0.6	35,254	32,259	38,103	30,335	25,376	20,156	26,031	24,340	26,691
A1.5W0.7	31,211	30,350	35,995	26,856	23,620	18,963	23,755	22,212	17,881
A1.5W0.8	27,506	27,984	33,474	23,668	21,521	17,485	21,032	19,666	16,457
A2.5W0.4	35,883	32,131	37,960	30,876	25,257	20,076	25,877	24,196	23,329
A2.5W0.5	33,183	30,863	36,555	28,553	24,087	19,283	24,360	22,777	23,992
A2.5W0.6	32,508	30,590	36,257	27,972	23,839	19,113	24,038	22,476	23,919
A2.5W0.7	34,326	32,125	37,953	29,536	25,251	20,072	25,869	24,189	23,612
A2.5W0.8	31,604	30,535	36,196	27,194	23,788	19,078	23,972	22,415	21,814
A3.5W0.4	29,278	28,444	33,956	25,193	21,922	17,772	21,552	20,152	22,329
A3.5W0.5	34,159	31,584	37,350	29,393	24,749	19,734	25,218	23,580	22,339
A3.5W0.6	31,761	30,724	36,404	27,329	23,961	19,197	24,196	22,624	20,973
A3.5W0.7	28,160	28,317	33,823	24,230	21,811	17,693	21,409	20,018	18,394
A3.5W0.8	26,544	27,204	32,666	22,840	20,847	16,998	20,159	18,850	14,127

The highest modulus of elasticity was obtained from the A1.5W0.6 mix. When the ratios of alkaline solutions increased the modulus of elasticity values decreased. According to AA/FA, the highest average elasticity was obtained from 0.6 ratio while the lowest average elasticity was 0.8 ratio. According to SS/SH, the highest average elasticity was obtained from 2.5 ratio, and the lowest average elasticity was 3.5 ratio in the study. The modulus of elasticity of the mixtures in which the heat-cured fly ash is activated with different ratios of activators are given in Fig. 6.

Concrete strength and density values were considered for the modulus of elasticity formulations developed by various researchers above and included in some regulations. The results obtained by using these formulations are given in Table 8. As seen from the results obtained, not only the compressive strength or additional density, but also the alkali activator solution ratios have some effects on the elastic modulus of the geopolymer concrete. Thus, a regression model was designed for the numerical calculation of the elastic modulus of the geopolymer concrete samples, and a formulation was developed by using the compressive strength and alkali activator ratios (SS/SH) and (AA/FA) for the analysis. The results obtained by using the formulation in Equation (20) are given in Fig. 7.

$$E = e^{\left(0.870\times ln(f_c)+1.24\times 10^{-5}\left[\left(\frac{SS}{SH}\right)\Big/\left(\frac{AA}{FA}\right)\right]^{4.5}+6.593\right)} \quad (20)$$

Regression statistics such as R, R^2, standard error and P values were calculated in order to reveal the accuracy of the regression model, which enables Eqs. (20) for the modulus of elasticity calculation, and whether the variables are related to each other. The values of regression statistics are presented in Table 9. It is observed that the model has a very low standard error, and the P values for the independent variables remained below 0.05. The R^2 value was obtained as a very close value to 0.80. The correlation coefficient R is above the value of 0.80, it is a measure of the good correlation between the variables [34,59].

It appears in Table 10 that the model proposed in the study yields closer results to the experimental data compared to other models by calculating RMSE values for all geopolymer concrete groups. In particular, R and R^2 values are around 0.80 mentioned in the literature, and P value is less than 0.05, which indicates that the independent variables used in the modulus of elasticity formulation are related to each other and the dependent variable and have a high correlation. According to the calculations, the results are both so close to the experimental data and yield better results than other formulations used in this study. Thus, it is found out that the use of alkali solution ratios in the formulation makes a positive contribution to the numerically calculated modulus of elasticity values.

3.4. Ductility

It was found out that GPC concrete shows more bending and softening behavior under axial loading compared to ordinary OPC concrete. Thus, it exhibits a more ductile behavior. This ductility is due to the presence of a higher amount of finer aluminosilicate particles in the GPC mixture [76,77]. Accordingly, the ductility of the mixtures in which low

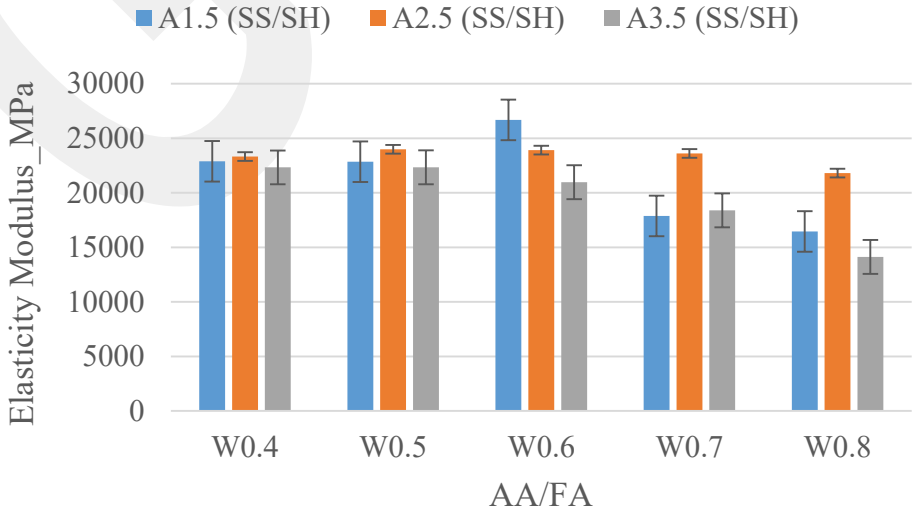

Fig. 6. Modulus of elasticity of mixtures using different ratios of solution.

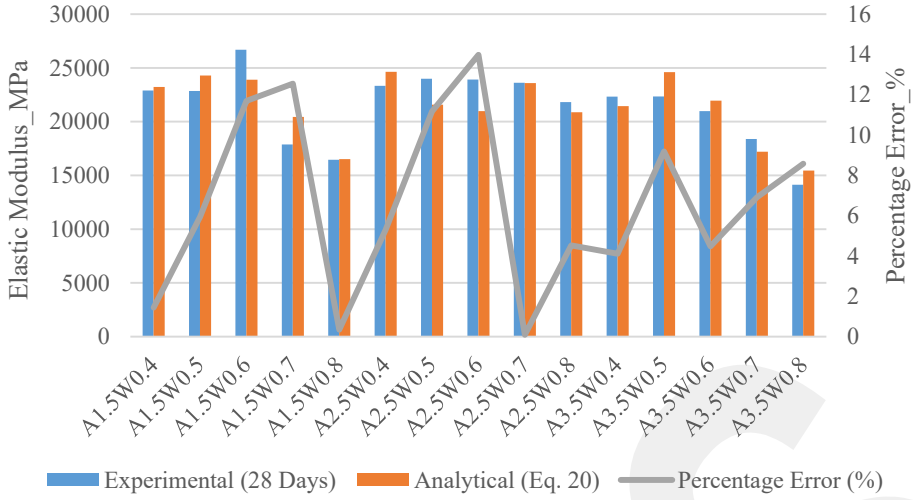

Fig. 7. Comparison of experimental and analytical modulus of elasticity and percent error values.

Table 9
Regression statistics values obtained for the Modulus of Elasticity formulation.

Regression Statistics	Values
Correlation Coefficient R	0.88
Determination Coefficient, R^2	0.77
Standard Error	0.088
P-value of Strength	4.48×10^{-5}
P-value of Alkali Solution	0.039
Sample Number	15

Table 10
RMSE values calculated by considering the error values of all samples of the empirical formulations used in the calculation of the modulus of elasticity.

Modulus of Elasticity	Diaz Loya et al.	Hardjito et al.	Lee-Lee	Nath-Sarker	Reddy-Muniraj	In this study
RMSE	33,49	18,89	15,03	18,32	13,11	7,93

calcium fly ash is activated with different ratios of activators is given in Fig. 8.

The highest ductility was obtained from the A3.5W0.7 mixture. By increasing the proportion of alkaline solutions, the ductility of the GPC samples increased. According to AA/FA, the highest ductility average was obtained from 0.7 ratio, and the lowest ductility average was 0.6 ratio. According to SS/SH, the highest ductility average was 3.5 ratio, and the lowest ductility was 1.5 ratio.

3.5. Stress- strain behavior of geopolymer concrete (GPC)

The stress-strain graphs were obtained from the experimental data of 15 different group GPC samples produced by activating low calcium fly ash with different ratios of activators. Then, the curves plotted by using the empirical σ-ε relations of the Hognestad, Kent-Park, Mander, Saatcioglu-Razvi unconfined concrete models are compared in Fig. 9. Accordingly, there are some differences between the graphs obtained from the experimental data and the curves calculated from the concrete models. These differences are expected in terms of results due to mathematical models and experimental data. Another factor leading to these differences is that the experimental graphics are plotted by calculating the averages of the σ-ε values of 3 samples for each group, as required by the standards. Therefore, the experimental curves are more linear than the curves calculated from the concrete models.

When the graphs are investigated, it appears that the peaks where the maximum stress is reached and the strain values where the rupture

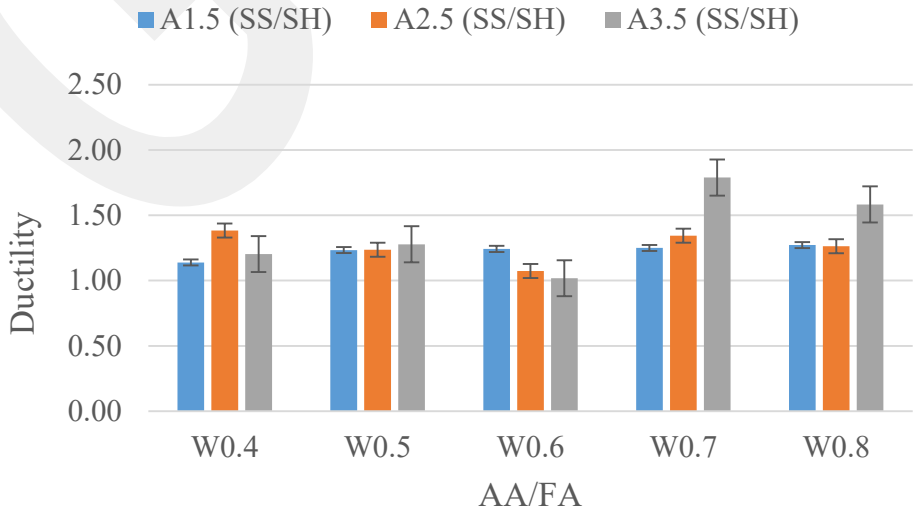

Fig. 8. The ductility values of the mixtures using different ratios of solution.

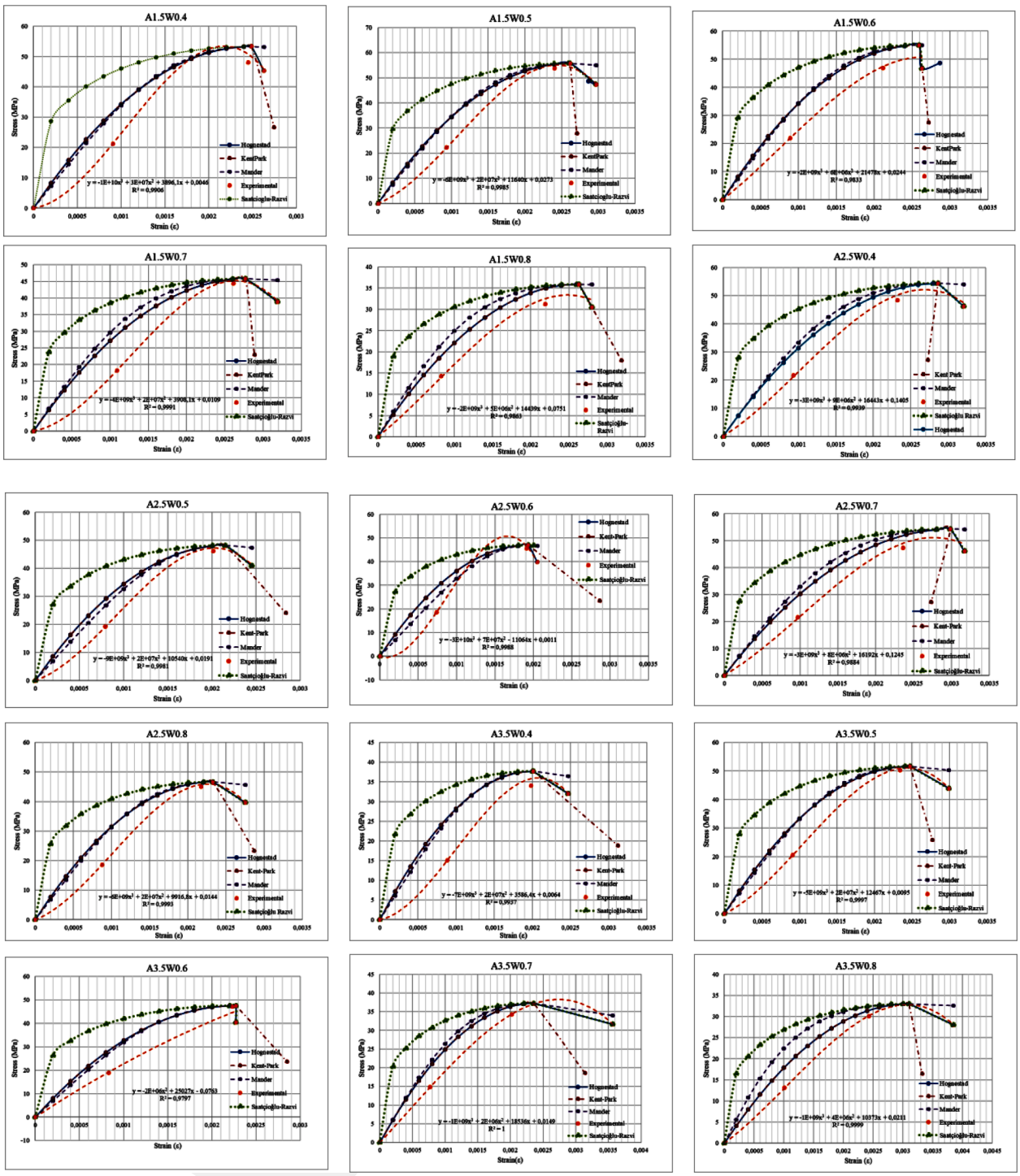

Fig. 9. Comparison of σ-ε graphs of different GPC concrete mix groups with σ-ε curves of concrete models.

occurs are compatible with each other. While the Saatcioglu-Razvi model is the most different graph with respect to the experimental data, Kent-Park and Hognestad are the most similar concrete models in terms of the graphs. Especially, the Hognestad model exhibits a very similar behavior with the descending slope after the peak of the curve. The Mander model, on the other hand, is a curve located between the nearest and farthest curves, and it has a different slope from the experimental data after the maximum stress value due to the empirical relations of the model. The curve of the Mander model located between the nearest and farthest curves has a different slope from the experimental data after the maximum stress value due to the empirical relations of the model. Thus, the Hognestad concrete model was the model that provides the most fitted stress-strain curves for geopolymer (GPC) concretes, among the most widely used unconfined OPC concrete models in the literature.

By making the evaluation on the stress strain graph, in general, the increase in the AA/FA ratio increased the strain, while decreased the strength. Similarly, the strain of the samples decreased, and the strength of the samples increased due to decrease in the AA/FA ratio, except the sample A2.5W0.7. On the other hand, the findings obtained from the changes in the AA/FA ratio for all SS/SH ratios validate this statement. When the effect of SS/SH ratios on stress strain behavior according to

AA/FA ratios are investigated the highest strength was obtained from samples with SS/SH ratio of 1.5 for AA/FA ratios of 0.4, 0.5 and 0.6 as well. The AA/FA ratio is 0.7 and 0.8, the samples with SS/SH ratio of 2.5 perform higher strength. The strains corresponding to the maximum stress also completely overlap with each other in terms of SS/SH ratio, except for the A3.5W0.8 sample. The lowest strength was obtained from the samples with SS/SH ratio of 3.5, except for the A2.5W0.5 sample. The highest values in terms of strain corresponding to the maximum stress were obtained from the samples with the SS/SH ratio of 1.5. Although the increase in the water/binder ratio for each of SS/SH ratios did not provide significant results in terms of stress, it resulted in an increase in strain. As the AA/FA ratio increased, the strain values corresponding to the maximum stress increased, especially for the SS/SH ratio of 3.5 with the ratio of AA/FA around 0.7 and 0.8. The unit weight of geopolymer concrete, maximum compressive strength and fracture pattern are similar to traditional concrete, however, behavior and ductility can change according to the change in alkaline ratio [78,79].

3.6. Consuming energy of geopolymer concrete (GPC)

The energy values consumed by the structural members under the load effects are associated with the ductility. Ductility is an important parameter in design, especially for structural members [51]. In this context, the amount of energy consumed by each sample was calculated by the areas under the σ-ε curves obtained from the average values of the experimental data [80]. The area under the σ − ε curve, which indicates the total energy per unit volume consumed by the sample is calculated by using the Equation (21);

$$U = \frac{1}{V}\int PdL = \int_0^L \frac{P}{Ao}\frac{dL}{Lo} = \int_0^\varepsilon \sigma(\varepsilon)d\varepsilon \tag{21}$$

where P is axial load, V is volume, Ao is cross-sectional area, and Lo is the length of the specimen. σ and ε represent the stress and strain values at any point on the stress-strain curves of geopolymer concrete, respectively. By calculating the areas under the curves drawn using concrete models, it was tried to determine the accuracy of the approaches of these models regarding the consumed energy. The amounts of consumed energy by the geopolymer concrete samples were calculated by using the experimental data and the values obtained from the analytical concrete models in order to evaluate the availability of these concrete models, which are used for traditional concrete, for geopolymer concrete samples and are presented in Table 11.

As seen in Table 11, the consumed energy values calculated from the concrete models are higher than those obtained from the experimental data, depending on the stress-strain curves, as expected. The energy values calculated from the Saatcioglu-Razvi concrete model have the maximum value in all groups. The lowest energy values are calculated with Hognestad for some samples, while it varies as Mander or Kent-Park for others. Since the groups are evaluated in general, the model that calculates the lowest amount of energy for a larger number of samples is Kent-Park. The reason is that the graph of this model generally proceeds with a lower slope up to the maximum stress value and then descends immediately and with a small slope after this point. Followed by the Kent-Park model, Mander is the model that yields the lowest energy value according to the number of samples. The reason is that the sample reaches the failure strain value in a short time after it reaches the maximum peak due to the nature of the model.

When the samples are evaluated according to their mixing ratios, Mander for W0.6 samples and Kent-Park concrete models for W0.7 samples provide the lowest energy values. The highest consumed energy value was calculated for the sample with A2.5W0.4 mixing ratio, while the lowest consumed energy value was obtained for the sample with A3.5W0.4 mixing ratio. The values of the experimental data and the values calculated from the concrete models were compared for the consumed energy by calculating the percentage error formulation, and these differences are given in Table 12.

As investigated the percentage error values in Table 12, it is seen that the highest difference was obtained from the Saatcioglu-Razvi model, as expected. On the other hand, the Kent-Park model gives very close results to the experimental data for some sample groups. Thus, it can be said that the Kent-Park model calculates closer results for a larger number of samples according to the overall number of groups. These results were followed by the Hognestad and Mander models. However, it should be noted that the values obtained from the Mander or Hognestad model are closer to the experimental values for some samples. The Kent-

Table 12
The differences of consuming energy of GPC for concrete models and experimental study (%).

Sample Name	Hognestad (%)	Kent-Park (%)	Saatcioglu-Razvi (%)	Mander et al. (%)
A1.5W0.4	32.30	36.87	62.41	32.30
A1.5W0.5	14.80	4.84	44.65	21.42
A1.5W0.6	38.74	28.28	53.89	24.27
A1.5W0.7	23.92	7.21	49.27	30.23
A1.5W0.8	19.43	35.69	46.46	27.17
A2.5W0.4	16.48	5.48	41.26	20.92
A2.5W0.5	22.27	39.14	47.07	19.94
A2.5W0.6	29.15	83.61	47.36	21.57
A2.5W0.7	17.89	2.05	44.86	23.27
A2.5W0.8	21.03	21.91	44.59	22.12
A3.5W0.4	31.17	61.71	55.18	31.31
A3.5W0.5	19.91	5.51	42.70	21.44
A3.5W0.6	28.09	64.90	59.32	25.97
A3.5W0.7	11.16	10.87	27.01	14.69
A3.5W0.8	12.04	9.21	33.03	23.43

Table 11
The amount of consuming energy of GPC from concrete models, regulations and experimental study (J).

Sample Name	Hognestad	Kent-Park	Saatcioglu-Razvi	Mander et al.	Experimental (28 Days)
A1.5W0.4	95227.93	98516.53	116903.68	95225.93	71978.65
A1.5W0.5	110363.93	100785.91	139064.77	116726.07	96137.53
A1.5W0.6	108205.40	100052.66	120024.46	96926.37	77994.29
A1.5W0.7	102268.56	88478.88	123185.71	107470.91	82525.93
A1.5W0.8	68572.11	77910.94	84090.10	73017.76	57416.71
A2.5W0.4	120849.96	98069.33	146560.28	125454.60	103751.82
A2.5W0.5	82306.70	93663.24	99002.37	80739.87	67317.52
A2.5W0.6	65394.86	92971.88	74615.37	61556.05	50635.80
A2.5W0.7	117342.35	97493.47	144192.73	122698.06	99537.05
A2.5W0.8	90501.23	91158.92	108115.11	91315.78	74775.63
A3.5W0.4	66324.55	81766.93	78466.17	66397.97	50564.38
A3.5W0.5	109694.29	96519.14	130540.82	111092.83	91478.40
A3.5W0.6	71777.82	92407.63	89278.99	70590.58	56038.80
A3.5W0.7	99957.82	80149.66	114214.36	103135.61	89926.21
A3.5W0.8	90806.99	73586.41	107815.93	100037.86	81047.40

Park concrete model presents closer results, of which the difference is maximum of 30 %, to the experimental data in terms of energy approach.

3.7. Performance comparison of geopolymer concrete

The effects of AA/FA and SS/SH ratios on the mechanical properties of geopolymer concrete according to the results acquired from the experimental study are listed as follows;

- As the AA/FA ratio increases, the compressive strength and the splitting tensile strength decreases. Accordingly, the optimum ratio was determined as 0.5. In terms of SS/SH ratio, the average compressive strength was obtained as 2.5>1.5>3.5.
- In cases where the AA/FA ratio exceeds 0.6 and the samples which have SS/SH ratio ranging from 1.5 to 3.5, a significant decrease in the modulus of elasticity was observed. Also, the optimum ratio was determined as 0.6. In terms of SS/SH ratio, the average elasticity modules were obtained as 2.5>1.5>3.5.
- Contrary to the strength and elasticity modulus, an increase in the AA/FA ratio increases the ductility. The ratio with the highest ductility was determined as 0.7. Similarly, the mean ductility values in terms of SS/SH ratio were obtained as 3.5>2.5>1.5.
- The calculation of energy consumption values based on the stress-strain curves enables both the evaluation of strength and ductility together. The highest energy consumption average for AA/FA was acquired from 0.7. The average energy consumption in terms of SS/SH ratio was obtained as 2.5>1.5>3.5.

As a result, the samples with SS/SH ratio of 2.5 are less affected than the samples with 1.5 and 3.5, regardless of the AA/FA ratio. Therefore, the samples with an SS/SH ratio of 2.5 are considered advantageous in terms of average values. A decrease in the AA/FA ratio increases the compressive and splitting tensile strength, while an increase increases the ductility and the energy consumed. The elastic modulus indicates that the optimum AA/FA ratio is 0.6 in terms of strength and ductility. The lowest and highest mechanical properties according to the mixing ratios of the geopolymer concrete samples are presented in Table 13.

As seen in Table 13, it is seen that the alkali activator ratios SS/SH and AA/FA affected the mechanical properties of the geopolymer concrete samples. Therefore, different from the formulations in the literature, two new formulations including AA/FA and SS/SH ratios are proposed for the analytical calculation of splitting tensile strength and modulus of elasticity. When compared with the experimental data and other formulations in the literature, it appears that the modulus of elasticity and splitting tensile strength values calculated with the help of these formulations provide very close results.

4. Conclusion

The effects of SS/SH and AA/FA ratios on the mechanical properties of a low calcium heat-cured fly ash geopolymer were investigated in this article. Comparisons of the research, regulations, existing concrete models and experimental data in the literature were made, and the similarities and differences of OPC and GPC were revealed. In the light of the data obtained from the experiments and analytical formulations were presented through the paper. When the stress-strain graphs obtained by using the models developed for OPC concrete behavior are investigated, it is seen that the peaks with maximum stress and strain values at rupture are compatible, although there are some differences in terms of curves. While the Saatcioglu-Razvi model provides the most different graph to the experimental data, the unconfined concrete models of Hognestad have the most similar graph.

As a result of evaluating the mechanical properties of geopolymer concrete according to the different activator and fly ash ratios; the best strength-strain relationship was obtained from 1.5 for AA/FA ratio 0.5 and 0.6, and SS/SH ratio 2.5 for AA/FA ratio 0.7. The reason for the segregation, which indicates a decrease in compressive strength in the mixtures of the samples with AA/FA ratios of 0.4 and 0.8, is presence of fly ash, which does not react sufficiently due to the bond formation between the products being reduced or not. Besides segregation, physical decomposition is also observed, and then the compressive strength is decreased as a mechanical result. During the production of the test samples, the samples with AA/FA ratio of 0.4 were not satisfactory in terms of workability, while the samples with AA/FA ratio of 0.8 were not found satisfactory in terms of consistency. In terms of ductility, samples with SS/SH ratio of 3.5 have the largest values for AA/FA ratios of 0.7 and 0.8. Although the samples with SS/SH ratio of 3.5 do not have as high compressive strength as the others (1.5–2.5), they have a reasonable strength for reinforced concrete structures and may find a use for themselves thanks to the advantage of ductility. For this reason, all SS/SH (1.5, 2.5, 3.5) ratios, which are the main topic of the research, and some AA/FA (0.5, 0.6, 0.7) ratios can be preferred in the production of geopolymer concrete. There was no significant relationship between strain and water/binder ratios. However, it can be said that the deformation increases in parallel with the water/binder ratio. It is observed that the water/binder ratio increases by the increase of the AA/FA ratio in the mixtures without any extra water addition, except for alkaline solutions, and it is more ductile in terms of deformation, which corresponds to the maximum stress, especially for the SS/SH ratio of 3.5. The findings of the study exhibit that the geopolymer concrete based on low calcium fly ash holds good potential for construction applications thanks to mechanical properties, reduced carbon emissions and sustainability characteristics.

New advances are still explored in geopolymer concrete with progress in technology. Future researches focus on the fire resistance of nanomaterial-based geopolymer concrete, 3D printing technology with geopolymer concrete, life cycle assessment of self-compacting and high-strength geopolymer concrete. However, the biggest challenge during the research was the short setting time, especially for the SS/SH 1.5 ratio. The improvement of the setting time can be addressed in future studies. In addition, it is evaluated that the volume and amount of concrete mixes made for production and the waiting time before and after heat curing affect the strength. Also geopolymer concrete can be tested for long term creep and shrinkage properties as an industrial product. Additional tests can be carried out to investigate all these effects or microstructural investigations on existing test samples can be made in order to better understand the chemical reactions during the activation of alkalis and benefit for future studies, which help to reduce time and material consumption. By determining the optimum SS/SH and AA/FA ratios after microstructural analysis, column behavior under uniaxial eccentric bending effect and four-point loading beam tests can be performed in further stages and the applicability of traditional reinforced concrete calculation and design in geopolymer concrete can be investigated. The transition from the material size to the bearing system size should be made with the help of the structural mechanics tests.

Table 13
Displaying the highest and lowest values according to the mixing ratios.

Mechanical Properties	SS/SH			AA/FA				
	1.5	2.5	3.5	0.4	0.5	0.6	0.7	0.8
Compressive Strength		+	–		+			–
Splitting Tensile Strength		+	–		+			–
Modulus of Elasticity		+	–			+		–
Ductility	–		+			–	+	
Consumed Energy		+	–			–	+	

+it shows maximum values and – it shows minimum values.

Declaration of Competing Interest

The authors declare that they have no known competing financial

interests or personal relationships that could have appeared to influence the work reported in this paper.

Acknowledgments

This research was supported by TUBITAK (The Scientific and Technological Research Council of Turkey) under grant number 121M236. We would like to thank ME-KA Ltd. Co., Mehmet Barut and Aydın Yüngeniş for their support in the Erciyes University Laboratory.

References

[1] Ma CK, Awang AZ, Omar W. Structural and material performance of geopolymer concrete: A review. Constr Build Mater 2018;186:90–102. https://doi.org/10.1016/j.conbuildmat.2018.07.111.
[2] Kamhangrittirong P, Suwanvitaya P, Suwanvitaya P, Chindaprasirt P. Synthesis and Properties of High Calcium Fly Ash. Proc. 36th Conf. Our World Concr. Struct., Singapore: 2011, p. 14–6.
[3] Unis Ahmed H, Mohammed AA, Mohammed AS. Compressive Strength of Geopolymer Concrete Composites: Modeling and Comprehensive Systematic Review. ResearchSquare 2021. https://doi.org/10.21203/RS.3.RS-611987/V1.
[4] Chi M, Huang R. Binding mechanism and properties of alkali-activated fly ash/slag mortars. Constr Build Mater 2013;40:291–8. https://doi.org/10.1016/j.conbuildmat.2012.11.003.
[5] Alghannam M, Albidah A, Abbas H, Al-Salloum Y. Influence of Critical Parameters of Mix Proportions on Properties of MK-Based Geopolymer Concrete. Arab J Sci Eng 2021;46:4399–408. https://doi.org/10.1007/s13369-020-04970-0.
[6] Sarkar M, Dana K. Partial replacement of metakaolin with red ceramic waste in geopolymer. Ceram Int 2021;47:3473–83. https://doi.org/10.1016/j.ceramint.2020.09.191.
[7] Mendes BC, Pedroti LG, Vieira CMF, Marvila M, Azevedo ARG, Franco de Carvalho JM, et al. Application of eco-friendly alternative activators in alkali-activated materials: A review. J Build Eng 2021;35:102010. https://doi.org/10.1016/j.jobe.2020.102010.
[8] de Azevedo ARG, Marvila MT, Ali M, Khan MI, Masood F, Vieira CMF. Effect of the addition and processing of glass polishing waste on the durability of geopolymeric mortars. Case Stud Constr Mater 2021;15:e00662. https://doi.org/10.1016/j.cscm.2021.e00662.
[9] Phoo-ngernkham T, Hanjitsuwan S, Damrongwiriyanupap N, Chindaprasirt P. Effect of sodium hydroxide and sodium silicate solutions on strengths of alkali activated high calcium fly ash containing Portland cement. KSCE J Civ Eng 2017;21:2202–10. https://doi.org/10.1007/s12205-016-0327-6.
[10] Özcan A, Karakoç MB. The Resistance of Blast Furnace Slag- and Ferrochrome Slag-Based Geopolymer Concrete Against Acid Attack. Int J Civ Eng 2019;17:1571–83. https://doi.org/10.1007/s40999-019-00425-2.
[11] Islam A, Alengaram UJ, Jumaat MZ, Bashar II. The development of compressive strength of ground granulated blast furnace slag-palm oil fuel ash-fly ash based geopolymer mortar. Mater Des 2014;56:833–41. https://doi.org/10.1016/j.matdes.2013.11.080.
[12] Zhang Z, Provis JL, Ma X, Reid A, Wang H. Efflorescence and subflorescence induced microstructural and mechanical evolution in fly ash-based geopolymers. Cem Concr Compos 2018;92:165–77. https://doi.org/10.1016/j.cemconcomp.2018.06.010.
[13] Koushkbaghi M, Alipour P, Tahmouresi B, Mohseni E, Saradar A, Sarker PK. Influence of different monomer ratios and recycled concrete aggregate on mechanical properties and durability of geopolymer concretes. Constr Build Mater 2019;205:519–28. https://doi.org/10.1016/j.conbuildmat.2019.01.174.
[14] Pimraksa K, Chindaprasirt P, Rungchet A, Sagoe-Crentsil K, Sato T. Lightweight geopolymer made of highly porous siliceous materials with various Na2O/Al2O3 and SiO2/Al2O3 ratios. Mater Sci Eng A 2011;528:6616–23. https://doi.org/10.1016/j.msea.2011.04.044.
[15] Panias D, Giannopoulou IP, Perraki T. Effect of synthesis parameters on the mechanical properties of fly ash-based geopolymers. Colloids Surfaces A Physicochem Eng Asp 2007;301:246–54. https://doi.org/10.1016/j.colsurfa.2006.12.064.
[16] Ravikumar D, Neithalath N. Effects of activator characteristics on the reaction product formation in slag binders activated using alkali silicate powder and NaOH. Cem Concr Compos 2012;34:809–18. https://doi.org/10.1016/j.cemconcomp.2012.03.006.
[17] Kumar S, Kumar R, Mehrotra SP. Influence of granulated blast furnace slag on the reaction, structure and properties of fly ash based geopolymer. J Mater Sci 2010;45:607–15. https://doi.org/10.1007/s10853-009-3934-5.
[18] Reddy MS, Dinakar P, Rao BH. Mix design development of fly ash and ground granulated blast furnace slag based geopolymer concrete. J Build Eng 2018;20:712–22. https://doi.org/10.1016/j.jobe.2018.09.010.
[19] Vora PR, Dave U V. Parametric studies on compressive strength of geopolymer concrete. Procedia Eng., vol. 51, No longer published by Elsevier; 2013, p. 210–9. https://doi.org/10.1016/j.proeng.2013.01.030.
[20] Görhan G, Kürklü G. The influence of the NaOH solution on the properties of the fly ash-based geopolymer mortar cured at different temperatures. Compos Part B Eng 2014;58:371–7. https://doi.org/10.1016/j.compositesb.2013.10.082.
[21] Nath P, Sarker PK. Flexural strength and elastic modulus of ambient-cured blended low-calcium fly ash geopolymer concrete. Constr Build Mater 2017;130:22–31. https://doi.org/10.1016/j.conbuildmat.2016.11.034.
[22] Karakoç MB, Türkmen I, Maraş MM, Kantarci F, Demirboła R, Ulur Toprak M. Mechanical properties and setting time of ferrochrome slag based geopolymer paste and mortar. Constr Build Mater 2014;72:283–92. https://doi.org/10.1016/j.conbuildmat.2014.09.021.
[23] Chithambaram SJ, Kumar S, Prasad MM. Thermo-mechanical characteristics of geopolymer mortar. Constr Build Mater 2019;213:100–8. https://doi.org/10.1016/j.conbuildmat.2019.04.051.
[24] Hardjito D, Rangan BV. Development and properties of low-calcium fly ash-based geopolymer concrete. 2005.
[25] Farooq F, Rahman SKU, Akbar A, Khushnood RA, Javed MF, Alyousef R, et al. A comparative study on performance evaluation of hybrid GNPs/CNTs in conventional and self-compacting mortar. Alexandria Eng J 2020;59:369–79. https://doi.org/10.1016/j.aej.2019.12.048.
[26] Viet Hung T, Duy Tien N, Van Dong D. Experimental study on section curvature and ductility of reinforced geopolymer concrete beams. Sci J Transp 2017;8:3–11.
[27] Ersoy U, Özcebe G. Reinforced Concrete. Ankara, Türkiye: Department of Civil Engineering Middle East Technical University; 2004.
[28] Hognestad E. A study on combined bending and axial load in reinforced concrete members. Illinois: 1951.
[29] Kent DC, Park R. Flexural Members with Confined Concrete. J Struct Div 1971;97:1969–90. https://doi.org/10.1061/JSDEAG.0002957.
[30] Mander JB, Priestley MJ, Park R. Observed stress-strain behavior of confined concrete. J Struct Eng 1988;114:1827–49.
[31] Mander JB, Priestley MJN, Park R. Theoretical stress-strain model of confined concrete. J Struct Eng 1988;114:1804–26.
[32] Saatcioglu M, Razvi S. Strength and Ductility of Confined Concrete 1992. https://doi.org/10.1061/(ASCE)0733-9445(1992)118:6(1590).
[33] Le HB, Bui QB, Tang L. Geopolymer Recycled Aggregate Concrete: From Experiments to Empirical Models. Mater 2021, Vol 14, Page 1180 2021;14:1180. https://doi.org/10.3390/MA14051180.
[34] Prachasaree W, Limkatanyu S, Hawa A, Sukontasukkul P, Chindaprasirt P. Manuscript title: Development of strength prediction models for fly ash based geopolymer concrete. J Build Eng 2020:32. https://doi.org/10.1016/J.JOBE.2020.101704.
[35] Thomas RJ, Peethamparan S. Alkali-activated concrete: Engineering properties and stress-strain behavior. Constr Build Mater 2015;93:49–56. https://doi.org/10.1016/J.CONBUILDMAT.2015.04.039.
[36] Bellum RR, Muniraj K, Madduru SRC. Empirical relationships on mechanical properties of class-F fly ash and GGBS based geopolymer concrete. Ann Chim Sci Des Mater 2019;43:189–97. https://doi.org/10.18280/acsm.430308.
[37] Srivathsav B, Kumar NP, Shrihari S, Vivek Kumar C. Proposed mathematical model for stress- strain behaviour of geopolymer concrete. E3S Web Conf 2021;309:01053. https://doi.org/10.1051/E3SCONF/202130901053.
[38] Wang H, Wang L, Li L, Cheng B, Zhang Y, Wei Y. The Study on the Whole Stress–Strain Curves of Coral Fly Ash-Slag Alkali-Activated Concrete under Uniaxial Compression. Mater 2020, Vol 13, Page 4291 2020;13:4291. https://doi.org/10.3390/MA13194291.
[39] Imtiaz L, Ur Rehman SK, Memon SA, Khan MK, Javed MF. A review of recent developments and advances in eco-friendly geopolymer concrete. Appl Sci 2020;10:1–56. https://doi.org/10.3390/app10217838.
[40] Standard A. C618–08a: Standard Specification for Coal Fly Ash and Raw or Calcined Natural Pozzolan for Use in Concrete. Pennsylvania, USA: West Conshohocken; 2008.
[41] ASTM C311. Standard Test Methods for Sampling and Testing Fly Ash or Natural Pozzolans for Use. vol. 04. Pennsylvania, USA: West Conshohocken. 2003.
[42] Garci Juenger MC, Jennings HM. Effects of high alkalinity on cement pastes. ACI Mater J 2001;98:251–5. https://doi.org/10.14359/10280.
[43] Sant G, Kumar A, Patapy C, Le Saout G, Scrivener K. The influence of sodium and potassium hydroxide on volume changes in cementitious materials. Cem Concr Res 2012;42:1447–55. https://doi.org/10.1016/j.cemconres.2012.08.012.
[44] Rangan BV. Studies on fly ash-based geopolymer concrete. Malaysian Constr Res J 2008;3:1–20.
[45] Palomo A, Grutzeck MW, Blanco MT. Alkali-activated fly ashes: A cement for the future. Cem Concr Res 1999;29:1323–9. https://doi.org/10.1016/S0008-8846(98)00243-9.
[46] Sathonsaowaphak A, Chindaprasirt P, Pimraksa K. Workability and strength of lignite bottom ash geopolymer mortar. J Hazard Mater 2009;168:44–50. https://doi.org/10.1016/j.jhazmat.2009.01.120.
[47] Swanepoel JC, Strydom CA. Utilisation of fly ash in a geopolymeric material. Appl Geochemistry 2002;17:1143–8. https://doi.org/10.1016/S0883-2927(02)00005-7.
[48] Hardjito D, Wallah S, Sumajouw D, Rangan B. Properties of Geopolymer Concrete with Fly Ash as Source Material: Effect of Mixture Composition. Spec Publ 2004;222:109–18. https://doi.org/10.14359/13308.
[49] Rattanasak U, Chindaprasirt P. Influence of NaOH solution on the synthesis of fly ash geopolymer. Miner Eng 2009;22:1073–8. https://doi.org/10.1016/j.mineng.2009.03.022.
[50] Mustafa Al Bakri AM, Kamarudin H, Binhussain M, Khairul Nizar I, Rafiza AR, Zarina Y. Microstructure study on optimization of high strength fly ash based geopolymer. Adv Mater Res 2012;476–478:2173–80. https://doi.org/10.4028/www.scientific.net/AMR.476-478.2173.

[51] Acar MC, Şener A, Özbayrak A, Çelik Aİ. The Effect of Zeolite Additive on Geopolymer Mortars. J Eng Sci Des 2020;8:820–32. https://doi.org/10.21923/JESD.768565.
[52] Hardjito D, Wallah SE, Sumajouw DMJ, Rangan BV. The stress-strain behaviour of fly ash-based geopolymer concrete. Dev Mech Struct Mater 2004;35:831–4.
[53] Lee NK, Lee HK. Setting and mechanical properties of alkali-activated fly ash/slag concrete manufactured at room temperature. Constr Build Mater 2013;47:1201–9. https://doi.org/10.1016/j.conbuildmat.2013.05.107.
[54] ACI318-14. 318-14: Building Code Requirements for Structural Concrete and Commentary. Farmington Hills, MI 48331, U.S.A.: 2014. https://doi.org/10.14359/51688187.
[55] Diaz-Loya EI, Allouche EN, Vaidya S. Mechanical properties of fly-ash-based geopolymer concrete. ACI Mater J 2011;108:300–6. https://doi.org/10.14359/51682495.
[56] Carino NJ, Lew HS. Re-examination of the Relation Between Splitting Tensile andCompressive Strength of Normal Weight Concrete. J Proc 1982;79:214–9. https://doi.org/10.14359/10900.
[57] Oluokun FA, Burdette EG, Deatherage JH. Splitting Tensile Strength and Compressive Strength Relationships at Early Ages. Mater J 1991;88:115–21. https://doi.org/10.14359/1859.
[58] Shanmugam BK, Vardhan H, Raj MG, Kaza M, Sah R, Hanumanthappa H. Experimentation and statistical prediction of screening performance of coal with different moisture content in the vibrating screen. Https://DoiOrg/101080/1939269920201767606 2020. https://doi.org/10.1080/19392699.2020.1767606.
[59] Cohen J. Statistical Power Analysis for the Behavioral Sciences. Stat Power Anal Behav Sci 2013. https://doi.org/10.4324/9780203771587.
[60] ASTM C39/C39M. Standard Test Method for Compressive Strength of Cylindrical Concrete Specimens 1. vol. i. Pennsylvania, USA: West Conshohocken. 2003.
[61] Ghugal YM, Patankar SV, Jamkar SS, Ghugal YM. Effect of water-to-geopolymer binder ratio on the production of fly ash based geopolymer concrete. ResearchgateNet 2013:2231–5721. https://doi.org/10.13140/2.1.4792.1284.
[62] Hadi MNS, Al-Azzawi M, Yu T. Effects of fly ash characteristics and alkaline activator components on compressive strength of fly ash-based geopolymer mortar. Constr Build Mater 2018;175:41–54. https://doi.org/10.1016/J.CONBUILDMAT.2018.04.092.
[63] ASTM. ASTM Standard C469: Standard Test Method for Static Modulus of Elasticity and Poisson's Ratio of Concrete in Compression. Pennsylvania, USA: West Conshohocken; 2010.
[64] Bellum R, Muniraj K, Matér SM-AC. undefined. Empirical relationships on mechanical properties of class-F fly ash and GGBS based geopolymer concrete. ResearchgateNet nd 2019.
[65] 363R-92 A. Aci 363R-92 Report on High Strength Concrete. 363R1–363R ed. Detroit: American Concrete Institute. 1992.
[66] CEB-FIP Code Model. Comite Euro-International du Beton. vol. 39. 1990.
[67] Gardner NJ, Poon SM. Time and Temperature Effects on Tensile, Bond, and Compressive Strengths. J Am Concr Inst 1976;73:405–9. https://doi.org/10.14359/11081.
[68] Raphael JM. Tensile Strength of Concrete. J Am Concr Inst 1984;81:158–65. https://doi.org/10.1007/978-3-642-41714-6_200519.
[69] de Larrard F, Malier Y. Engineering Properties of Very High Performance Concretes. High Perform Concr 2018:85–114. https://doi.org/10.1201/9780203752005-6.
[70] Ryu GS, Lee YB, Koh KT, Chung YS. The mechanical properties of fly ash-based geopolymer concrete with alkaline activators. Constr Build Mater 2013;47:409–18. https://doi.org/10.1016/j.conbuildmat.2013.05.069.
[71] ASTM C 469/C 496M. Standard Test Method for Splitting Tensile Strength of Cylindrical Concrete Specimens. Pennsylvania, USA: West Conshohocken; 2004.
[72] Sofi M, van Deventer JSJ, Mendis PA, Lukey GC. Engineering properties of inorganic polymer concretes (IPCs). Cem Concr Res 2007;37:251–7. https://doi.org/10.1016/J.CEMCONRES.2006.10.008.
[73] Fernández-Jiménez AM, Palomo A, López-Hombrados C. Engineering properties of alkali-activated fly ash concrete. ACI Mater J 2006;103:106–12. https://doi.org/10.14359/15261.
[74] Olivia M, Nikraz H. Properties of fly ash geopolymer concrete designed by Taguchi method. Mater Des 2012;36:191–8. https://doi.org/10.1016/j.matdes.2011.10.036.
[75] TS-500. Requirements for design and construction of reinforced concrete structures. Ankara, Türkiye: 2000.
[76] Ganesan N, Indira PV, Santhakumar A. Prediction of ultimate strength of reinforced geopolymer concrete wall panels in one-way action. Constr Build Mater 2013;48:91–7. https://doi.org/10.1016/j.conbuildmat.2013.06.090.
[77] Hassan A, Arif M, Shariq M. A review of properties and behaviour of reinforced geopolymer concrete structural elements- A clean technology option for sustainable development. J Clean Prod 2020;245:118762. https://doi.org/10.1016/j.jclepro.2019.118762.
[78] Çelik Aİ, Özbayrak A, Şener A, Acar MC. Effect of Activators in Different Ratios on Compressive Strength of Geopolymer Concrete. Can J Civ Eng 2022. https://doi.org/10.1139/CJCE-2021-0529.
[79] Çelik Aİ, Özbayrak A, Şener A, Acar MC. Numerical analysis of flexural and shear behaviors of geopolymer concrete beams. J Sustain Constr Mater Technol 2022;7:70–80. https://doi.org/10.47481/JSCMT.1116561.
[80] Chitrala S, Jadaprolu GJ, Chundupalli S. Study and predicting the stress-strain characteristics of geopolymer concrete under compression. Case Stud Constr Mater 2018;8:172–92. https://doi.org/10.1016/J.CSCM.2018.01.010.